Analysis of three sets of SWIW tracer-test data using a two-population complex fracture model for matrix diffusion and sorption

Christine Doughty[1] and Chin-Fu Tsang[1, 2]

[1]Earth Sciences Division
Lawrence Berkeley National Laboratory
Berkeley, California 94720, USA

[2]Department of Earth Science and Engineering
Imperial College London, SW7 5JP, UK

July 2009

Abstract

A complex fracture model employing two populations for diffusion and sorption is proposed to analyze three representative single-well injection-withdrawal (SWIW) tracer tests from Forsmark and Laxemar, the two sites under investigation by the Swedish Nuclear Fuel and Waste Management Company (SKB). One population represents the semi-infinite rock matrix and the other represents finite blocks that can become saturated, thereafter accepting no further diffusion or sorption. The diffusion and sorption parameters of the models are inferred by matching tracer breakthrough curves (BTCs). Three tracers are simultaneously injected, uranine (Ur), which is conservative, and rubidium (Rb) and cesium (Cs), which are non-conservative. For non-sorbing tracer uranine, the finite blocks become saturated with test duration of the order of 10 hours, and both the finite and the semi-infinite populations play a distinct role in controlling BTCs. For sorbing tracers Rb and Cs, finite blocks do not saturate, but act essentially as semi-infinite, and thus BTC behavior is comparable to that obtained for a model containing only a semi-infinite rock matrix. The ability to obtain good matches to BTCs for both sorbing and non-sorbing tracers for these three different SWIW data sets demonstrates that the two-population complex fracture model may be a useful conceptual model to analyze all SWIW tracer tests in fractured rock, and perhaps also usual multi-well tracer tests. One of the two populations should be semi-infinite rock matrix and the other finite blocks that can saturate. The latter can represent either rock blocks or gouge within the fracture, a fracture skin zone, or stagnation zones.

1. Introduction

The usual conceptual model of flow and transport through fractured rock involves advection and dispersion of solutes or tracers through the fracture network coupled with diffusion and sorption into the surrounding rock matrix. In a single-well injection-withdrawal (SWIW) tracer test (Haggerty et al., 2001; Schroth et al., 2001; Nordqvist and Gustafsson, 2002; 2004, Gouze et al., 2008), one well injects fluid and tracer at a constant rate for a period of time, followed by injection of fluid (chase fluid) without tracer for a somewhat longer period. Then the pump is reversed and the well withdraws fluid at the same rate until most or all of the tracer is recovered. SWIW tests have also been referred to as push-pull and huff-puff tests (Tsang, 1995; Haggerty et al., 1998). Unlike typical two-well tracer tests, SWIW tests, involving reversing flow fields by injection and subsequent withdrawal at the same flow rate, focus on diffusion and sorption, and the test results are ideally independent of advective heterogeneity ("advective dispersivity"), channeling, and flow dimension.

For two-well tracer migration, key features of a tracer breakthrough curve (BTC) are the peak arrival time t_{pk}, the peak height C_{pk}, the slope of the tail, and the time t_0 of the tracer "first" arrival (e.g., when $C \approx 10^{-3} \cdot C_{pk}$). For a SWIW test, they are peak height, slope of tail, and the tracer recovery factor. Travel time is essentially fixed for a SWIW test, set by the schedule of the test, whereas travel distance is essentially fixed for a two-well test, set by well separation. Figure 1 shows a schematic view of tracer particles moving through a fractured medium for a two-well test and for a SWIW test, and the opportunities they experience for diffusion and sorption into the surrounding rock matrix. In a two-well test, particles always see new rock matrix, whereas in a SWIW test, they revisit the same rock matrix on the withdrawal phase that they already passed during the injection phase. If this rock matrix is composed of finite-sized blocks, these blocks may become saturated in a SWIW test, thus greatly inhibiting further diffusion and sorption. Compared to a typical two-well tracer test, a SWIW test is expected to produce a higher tracer recovery, be more feasible in the field, and possibly provide information on the flow wetted surface (FWS) of a fracture network (Tsang and Doughty, 2009).

The present paper uses complex fracture models (Tsang and Doughty, 2003, 2009) containing two rock populations for diffusion and sorption to model three representative SWIW tests conducted at Forsmark and Laxemar, the two sites currently under investigation by the Swedish Nuclear Fuel and Waste Management Company (SKB). For tracers, the tests used uranine (Ur), a non-sorbing tracer, and rubidium (Rb) and cesium (Cs), which are sorbing tracers. By calibrating the models to the BTCs obtained in the field, diffusion and sorption parameters for the two populations are obtained. The next section, Section 2, briefly presents the complex fracture model. Section 3 then describes the field data, followed by results of the model calibration in Section 4. Section 5 discusses some of the features that make the modeling challenging, and Section 6 provides some conclusions.

.

2. Model Features

In this section, we briefly describe the complex fracture model (Tsang and Doughty, 2003, 2009). The complex fracture model for fluid flow and tracer transport incorporates the important physical effects of a realistic fracture, as illustrated in Figure 2. As originally formulated, the complex fracture model is composed of two sub-fractures, and the flow through the fracture q is the sum of the flow through the two sub-fractures, q_1 and q_2:

$$q = q_1 + q_2. \tag{1}$$

The flows q_1 and q_2 are related by

$$q_2 = \alpha\, q_1, \tag{2}$$

where α can range from 0 (only a single sub-fracture) to 1 (two identical sub-fractures).

The transmissivity over the fracture plane is assumed to be heterogeneous: $T(x,y)$. The fracture aperture distribution is also heterogeneous, with aperture $b(x,y)$ related to $T(x,y)$ through the cubic law.

In general, the complex fracture model assumes two or more sub-fractures and possible diffusion and sorption into three populations: fracture-filling gouge, small altered rock matrix blocks within the fracture zone, and unaltered semi-infinite rock matrix on both sides of the fracture. For the present study, however, only one sub-fracture is used and two populations for diffusion and sorption are considered: one finite-block population representing gouge and small altered blocks, and one semi-infinite population representing intact rock matrix on both sides of the fracture plane.

In this two-population model, the parameters characterizing the transport are fracture aperture, matrix porosity ϕ_m, and effective matrix diffusion coefficient D_e, which is defined as the product of free-water diffusion coefficient, matrix tortuosity τ, and matrix porosity ϕ_m. For a sorbing tracer, the product of rock density ρ_p and sorption coefficient K_d replaces ϕ_m where it appears as an independent parameter, but not within D_e. Each of the two populations has its own values of ϕ_m, τ, and $\rho_p K_d$, with its own characteristic length scale. For the finite population, the characteristic length scale is denoted $2r_m$, and represents the size of the finite block. For the semi-infinite population, the characteristic length scale is the fracture aperture b.

A numerical model is used to simulate the fluid flow field through a two-dimensional fracture based on a finite-difference method using a rectangular grid. The central portion of the model, where the well is located and where the tracer is expected to remain, has high spatial resolution. Beyond this region, the model becomes coarser, and extends a great distance to constant-pressure boundaries. Then a particle-tracking algorithm is used to calculate tracer advection through the fracture, including the distribution of particles among sub-fractures. Diffusion and sorption into the different populations making up the surrounding rock matrix are determined probabilistically by inverting semi-analytical

solutions (Tsang and Tsang, 2001; Tsang and Doughty, 2003) to determine delay times that represent diffusion and sorption.

In order to minimize numerical dispersion that occurs while calculating advective transport in the fracture plane, we employ a special procedure for modeling the flow reversal that happens during a SWIW test. During the injection period the advection calculation is normal — particle advection from one cell to its neighboring cells occurs based on the finite-difference calculation of the flow velocities between these cells. If the flow direction is not parallel to the grid orientation, the destination cell is chosen probabilistically from among all the neighboring cells, with probability proportional to the flow rate into each cell. For each particle, the sequence of cells traversed is recorded. Then, for advection during the withdrawal period, the sequence of cells traversed by the particle during injection is reversed. Thus, the advective part of transport occurring during the injection period is exactly reversed for the withdrawal period, properly simulating the physical situation. Diffusion and sorption still occur probabilistically by inverting semi-analytical solutions as described above.

Over the course of the development of the complex fracture model, three different conceptual models, C1, C2 and C3, have been considered to describe how the different populations operate relative to each other. In conceptual model C1 (Tsang and Doughty, 2003), for each particle at any given time step, diffusion and sorption occur into only one of the three populations, chosen probabilistically (sum total of probability being unity) based on given proportions of each population. This conceptualization implies that all populations block each other. Thus, when finite populations saturate, the particle does not have an opportunity to diffuse into the semi-infinite medium instead. Conceptual model C2 (Tsang et al., 2008) considers two-level diffusion. At the first level, each particle chooses one of two finite populations probabilistically ($\Sigma P \leq 1$) and a tentative delay time t_1 is calculated. At the second level, diffusion into the semi-infinite medium is calculated and a second tentative delay time t_2 is obtained. We then take the maximum of t_1 and t_2. This conceptualization implies that only the two finite populations block each other. When finite populations saturate, the particle does have an opportunity to diffuse

into the semi-infinite medium instead. The conceptual model C2 has the advantage over C1 in that the tracer BTCs tend to the semi-infinite case for large times, when the finite blocks are saturated.

Conceptual model C3, proposed by Tsang and Doughty (2009), is the approach used in the present paper. In this model, each particle sees each of the two populations at each time step weighted by its own effective contact area. Taking the effective contact area with the semi-infinite matrix to be unity, the effective contact areas for the finite population is less than one. Delay times for the two populations are then summed. This conceptualization implies that neither population blocks the other. Each particle always has the opportunity to diffuse into both populations. This conceptual model not only yields the semi-infinite results at large times after the saturation of the finite blocks, but also provides the possibility of representing, at least approximately, the multi-layer effect of tracer migration into the semi-infinite matrix after passing through rock of a finite thickness.

Now the model is applied to calculate tracer flow and transport. The BTC is obtained by binning particle arrivals to form a histogram. If n particles arrive in bin i of time-duration $\Delta t(i)$, they correspond to a dimensionless concentration $C_{bin}(i)/C_{in}$ given by

$$\frac{C_{bin}(i)}{C_{in}} = \frac{n(i)/\Delta t(i)}{N/t_{inj}}, \tag{3}$$

where N is the total number of particles injected (typically of the order of 200,000), t_{inj} is the duration of the injection period, and C_{in} is the injection concentration, given by $C_{in} = IM/V_{bh}$, where IM is the injected mass and V_{bh} is the volume of the borehole section into which tracer is injected. Bin time duration (i.e., bin width) increases with time to more efficiently handle BTC with long tails. The time corresponding to bin i is given by

$$t(i) = \sum_{j=1}^{i-1} \Delta t(j) + \Delta t(i)/2 . \tag{4}$$

Rearranging Equation (3) for dimensionless concentration yields

$$C_{bin}(i) = \frac{n(i)/\Delta t(i)}{N/t_{inj}} \frac{IM}{V_{bh}}. \quad (5)$$

$C_{bin}(i)$ is then modified to explicitly include borehole mixing according to

$$C_{bh}(i) = \frac{V_{bh}C_{bh}(i-1) + V_{bin}(i)C_{bin}(i)}{V_{bh} + V_{bin}(i)}, \quad (6)$$

where $C_{bh}(i)$ is the mixed concentration in the borehole for bin i and $V_{bin}(i)$ is the volume of fluid extracted during time interval $\Delta t(i)$. A dummy is inserted into the borehole to minimize V_{bh}, and thus minimize the difference between C_{bin} and C_{bh}.

Table 1 summarizes the parameters used to generate the stochastic fracture transmissivity distribution (Deutsch and Journel, 1988) for the present study, which are representative of a tracer test site in granitic rock at Äspö, Sweden (Doughty and Uchida, 2005) and thus correspond to realistic field properties. Figure 3 shows the resulting hydraulic conductivity distribution. The transmissivity and fracture aperture values are comparable to values estimated for the Forsmark site (Thur et al., 2007a; 2007b). Recent studies (Tsang and Doughty, 2009) have shown that SWIW-test BTCs are not very sensitive to the heterogeneity level of the transmissivity distribution. Table 2 summarizes the initial diffusion and sorption parameters for the model. Values shown in bold are varied during calibration to the BTCs observed in the field.

3. Field Data

Field data from three SWIW tracer tests conducted by Swedish Nuclear Fuel and Waste Management Company (SKB) were proposed for our analysis (Geier, private communications, 2008). They were selected as representative of a range of possible BTC

profiles found in a series of SWIW tracer tests that were performed by SKB in the past few years. Specifically the three data sets are from the SWIW test in a well at Laxemar, KLX11A, borehole section 598-599 m, and from two SWIW tests in a well at Forsmark, KFM01D, borehole sections 431-432 m and 377-378 m. Table 3 summarizes the operating conditions for each SWIW test modeled. In each of the SWIW tests, the tracer injection period is modeled as having a constant flow rate. Following tracer injection, there is a chase-fluid injection period, also modeled with a constant flow rate. Next is a waiting period in which no flow occurs, followed by withdrawal at a constant flow rate. In these tests, some of the tracers are already present in the formation fluid prior to the SWIW tests, giving rise to a background level that needs to be subtracted from the BTC.

With tracer injected at a constant concentration C_{in}, the concentration C entering the fracture has a time-dependent concentration due to mixing in the borehole. It can be calculated according to

$$C(t) = (C_0 - C_{in})\exp[-Qt/(V_{bh} + K_a A_{bh})] + C_{in} \quad \text{for} \quad 0 < t < t_{inj} \tag{7a}$$

$$C(t) = C(t_{inj})\exp[-Q(t - t_{inj}) /(V_{bh} + K_a A_{bh})] \quad \text{for} \quad t > t_{inj}, \tag{7b}$$

where surface sorption coefficient K_a = 0.01 for Cs and Rb and 0 for Ur, C_0 = 0 (no tracer initially in borehole), V_{bh} is borehole volume, A_{bh} is borehole surface area, and Q is injection rate. Figure 4 illustrates the effect of the time-dependent tracer concentration.

Figure 5 shows the tracer BTC field data for the three SWIW tests, having included the necessary background concentration corrections. In the BTC plots, concentration C (in mg/L) is normalized by the injected mass IM (in mg).

4. **Model Results**

For each SWIW test, the uranine BTC was considered first, with matrix porosity ϕ_m for the finite and infinite populations, and characteristic length scale $2r_m$ for the finite

population varied until a reasonable match was obtained. Then these same parameter values were used for the Rb and Cs BTC, and their respective sorption coefficient $K_d\rho_p$ were varied until a reasonable match was obtained. BTC results are shown in Figure 5 and the corresponding property values are shown in the upper section of Table 4. The matches for KLX11A and KFM01D 431 are very good. The match for KFM01D 377 is relatively less good for Ur and Rb, and further considerations of variability within our conceptual model may be worthwhile.

5. Discussion

5.1 Background Concentration

Having to subtract a background concentration to obtain BTC means that the lowest values in the BTC (very early and very late times) are rather inaccurate, because they are the result of subtracting two very small numbers from one another. This is illustrated in Figure 5b (with large and small green symbols), which shows that two alternative uranine background values of .019 and 0.048 mg/L yield very different BTC tails. The former background value is considered more accurate and is used in present data analysis; the latter is a larger value that appeared in preliminary data reports. Hence, when calibrating model parameters, little weight is attached to the very end of the uranine BTC. On the other hand, this observation also implies the need to measure background concentration levels with a high degree of accuracy.

5.2 Use of Semi-infinite Only Model for Analysis

In general, the tails of the BTC for uranine show more variability than do those for Rb and Cs. This reflects the distinct way the semi-infinite and finite populations respond to SWIW tracer migration. Generally, matrix porosity is much bigger for the finite population than for the semi-infinite population. Because matrix porosity is one of the components of the effective diffusion coefficient, small matrix porosity corresponds to a weak diffusion coefficient. Thus, diffusion is primarily controlled by the finite

population, with a weak contribution from the semi-infinite population. In particular, the finite population provides more initial opportunity for diffusion, but once it saturates, diffusion into the semi-infinite population becomes the dominant factor.

In a supplementary study, we attempt to fit the KFM01D-431 data with a model containing only the semi-infinite population for diffusion and sorption. Figure 6 shows the fitted BTC, and the lower section of Table 4 shows the corresponding diffusion properties. The curve labeled "Ur model" uses the ϕ_m value from Table 4 and does an adequate job of matching the late-time portion of the BTC tail, but significantly over-predicts peak height. The curve labeled "Alt. Ur model" is obtained by increasing ϕ_m to obtain a better fit to the peak height, which results in a poor fit to the BTC tail. Note that for non-sorbing uranine, neither single- population model successfully matches the entire uranine BTC, whereas for sorbing Rb and Cs, single-population models yield just as good a match as do two-population models (see Figure 5b).

For all three SWIW tests considered, the Cs BTCs show a linear tail with a slope (on a log-log plot) close to -3/2, which is a characteristic of diffusion into a semi-infinite medium. It turns out that all the Cs BTCs can be equally well matched using only a single population for diffusion and sorption (as shown in Figure 6 for KFM01D 431). Furthermore, that population can be either finite or semi-infinite. This is because Cs sorption is so large that even the finite population has a large capacity for uptaking Cs, and thus acts essentially semi-infinite.

The one Rb BTC that does not show a linear tail with a -3/2 slope is that for KFM01D 377 (see Figure 5c). Taken alone, this tail suggests that just as for uranine, both finite and semi-infinite populations play a role in controlling the Rb BTC. However, the other two Rb BTCs are quite similar to the Cs BTCs and hence the inferred sorption coefficients for Rb are comparable to those of Cs, implying that Rb uptake is comparable to Cs uptake. This in turn implies that the Rb BTC tails should all be linear, which is clearly not the case for KFM01D 377. We have limited our discussion of BTC behavior

within the framework of the complex fracture model, but there may be some other features impacting this BTC that have not yet been accounted for.

6. Concluding Remarks

Three representative SWIW tracer tests recently conducted by SKB have been analyzed with a complex fracture model employing two populations for diffusion and sorption, one population being the semi-infinite rock matrix and the other, finite blocks. The results show that by adjusting diffusion and sorption parameters of the model, a good match with field data is obtained for BTCs of both conservative and non-conservative tracers simultaneously. For non-sorbing tracer uranine, both the finite and the semi-infinite populations play a distinct role in controlling BTC. At early times (the tracer peak) the finite population is most important, but at later times (the tracer tail), the finite population becomes saturated and the semi-infinite population controls the BTC. In contrast, for sorbing tracers Rb and Cs, the finite population does not saturate so a single-population model can be used to match these BTCs. Hence, to match the behavior of both non-sorbing and sorbing tracers, two populations, one finite and the other semi-infinite, are required to capture all the features of the BTCs.

The conclusion of this study using the three representative SWIW data sets shows that the two-population complex fracture model may be a useful conceptual model to analyze all SWIW tracer tests in fractured rock and perhaps also usual multi-well tracer tests. One of the two populations should be semi-infinite rock matrix and the other finite blocks that can saturate. The latter can represent either rock blocks within the fracture, a fracture skin zone, or stagnation zones.

Acknowledgements

We thank Joel Geier, Georg Lindgren, and Kenzi Karasaki for their reviews of this paper, and we are grateful to Joel Geier and Peter Andersson for providing insights into the field data. The second author has benefitted greatly through discussions with the members of the INSITE Core Group and the staff of SSM (formerly SKI). This work was jointly

supported by Swedish Radiation Safety Authority (SSM), and Japan Atomic Energy Agency (JAEA) under the Bi-national Research Cooperation Program between JAEA and the U.S. Department of Energy. The work was performed under the auspices of the U.S. Department of Energy through Contract No. DE-AC02-05CH11231.

References

Cvetkovic, V., H. Chen, and J.-O. Selroos, First TRUE Stage: Evaluation of tracer retention understanding experiments (first stage) at Äspö, *Rep. ICR-00-01*, Swedish Nuclear Fuel and Waste Management Co. (SKB), Stockholm, Sweden, 2000.

Deutsch, C.V. and A.G. Journel, GSLIB: *Geostatistical software library and user's guide*, 2nd ed., Oxford Univ. Press, New York 1998.

Doughty, C. and M. Uchida, PA calculations for feature A with third-dimension structure based on tracer test calibration, *Rep. IPR-04-33*, Swedish Nuclear Fuel and Waste Management Co. (SKB), Stockholm, 2003.

Gouze, P., T. Le Borgne, R. Leprovost, G. Lods, T. Poidras, and P. Pezard, Non-Fickian dispersion in porous media: 1. Multiscale measurements using single-well injection withdrawal tracer tests, Water Resour. Res., 44, W06426, doi:10.1029/2007WR006278, 2008.

Haggerty, R., S.W. Fleming, L.C. Meigs, S.A. McKenna, Tracer tests in fractured dolomite. 2. Analysis of mass-transfer in single-well injection-withdrawal tests. Water Resources Research 37, no. 5: 1129-1142, 2001.

Haggerty, R., M.H. Schroth, and J.D. Istok, Simplified method of "push-pull" test data analysis for determining in situ reaction rate coefficients. *Ground Water* 36(2), 314-324, 1998.

Mazurek, M., P. Bossart and J. Hermanson, Classification and characterization of water-conducting features at Äspö., *Proc. Intern. Seminar First TRUE Stage,* Äspö Hard Rock Laboratory, Sweden, September 9-11, 2000, pp. 203-208; published as *Rep. TR-01-24*, Swedish Nuclear Fuel and Waste Management Co. (SKB), Stockholm, Sweden, 2001.

Nordqvist, R., and E.Gustafsson, Single-well injection-withdrawal tests (SWIW). Literature review and scoping calculations for homogeneous crystalline bedrock conditions. SKB R-02-34, Swedish Nuclear Fuel and Waste Management Co. (SKB), Stockholm, Sweden, 2002.

Nordqvist, R. and E.Gustafsson, Single-well injection-withdrawal tests (SWIW). Investigation and evaluation aspects under heterogeneous crystalline bedrock

conditions. SKB R-04-57. Swedish Nuclear Fuel and Waste Management Co. (SKB), Stockholm, Sweden, 2004.

Schroth, M.H., J.D. Istok, R. Haggerty, In situ evaluation of solute retardation using single-well push-pull test. Advances in Water Resources 24: 105-117, 2001.

Thur, P., R. Nordqvist, and E. Gustafsson, Forsmark site investigation: Groundwater flow measurements and SWIW tests in borehole KFM01D, *Rep. P-07-52*, Swedish Nuclear Fuel and Waste Management Co. (SKB), Stockholm, Sweden, 2007a.

Thur, P., R. Nordqvist, E. Gustafsson, Oskarshamn site investigation: Groundwater flow measurements and SWIW tests in borehole KLX11A, *Rep. P-07-180*, Swedish Nuclear Fuel and Waste Management Co. (SKB), Stockholm, Sweden, 2007b.

Tsang, C.-F. and C. Doughty, A particle-tracking approach to simulating transport in a complex fracture, *Water Resources Research*, **39**(7), 1174, doi:10.1029/2002WR001614, 2003.

Tsang, C.-F. and C. Doughty, Insight from simulations of single-well injection-withdrawal tracer tests on simple and complex fractures, Rep. LBNL-2487E, Lawrence Berkeley National Laboratory, Berkeley, CA, 2009.

Tsang, C.-F., C. Doughty, and M. Uchida, Simple model representations of transport in a complex fracture and their effects on long-term predictions, *Water Resources Research*, **44**, W08445, doi:10.1029/2007WR006632, 2008.

Tsang, Y. W. Study of alternative tracer tests in characterizing transport in fractured rocks, *Geophysical Research Letters*, **22**(11), 1421–1424, 1995.

Tsang, Y.W. and C.F. Tsang, A particle-tracking method for advective transport in fractures with diffusion into finite matrix blocks, *Water Resources Research*, **37**(3), 831-835, 2001.

List of Tables

List of Figures

Table 1. Parameters of fracture transmissivity distribution (Doughty and Uchida, 2003).

Parameter	Value
Fracture dimensions (m)	30, 30, 0.01
nx, ny, nz (number of grid blocks in central portion of model)	150, 150, 1
Δx, Δy, Δz (m) (grid spacing in central portion of model)	0.20, 0.20, 0.01
Sequential indicator simulation using a CDF for $\log_{10}T$ based on 15 well-test analyses for 5 boreholes	
Geometric mean transmissivity T	$3.56 \cdot 10^{-7}$ m^2/s
Standard deviation of $\log_{10}T$ (T in m^2/s)	1.35
Mean fracture aperture b (from cubic law)	$7.54 \cdot 10^{-5}$ m
Spherical variogram range for lower 80% of T values	0.6 m
Spherical variogram range for higher 20% of T values	2 m

Table 2. Diffusion parameters for finite and semi-infinite rock populations. Values shown in bold are varied during model calibration.

Parameter	Finite population (altered rock inside fracture)	Semi-infinite matrix (unaltered rock outside fracture plane)
Matrix porosity ϕ_m (-)	**0.04**	**0.004**
Characteristic length (m)	$2r_m$ = **0.005**	$b = 7.54 \cdot 10^{-5}$
D_e (m^2/s)	$3 \cdot 10^{-12}$	$1.2 \cdot 10^{-13}$
Effective contact area (-)	**0.2**	1.0
Rb $K_d \rho_p$ (-)	**8.4**[*]	**1**[*]
Cs $K_d \rho_p$ (-)	**116**[*]	**16**[*]

[**]From Cvetkovic et al., 2000

Table 3. Test schedules for the three SWIW tests modeled.

Test	Start time (hr)	Flow Rate (L/hr)	Injected Mass (mg) Injection Concentration (mg/L) Background Correction (mg/L)		
			Ur	Rb	Cs
KLX11A 598					
Injection	0	9.2	942	1610	697
Chase	0.8	9.7	122.3	209.1	90.5
Rest	9.9	0	0.03	0	0
Withdrawal	11.73	9.4			
KFM01D 431					
Injection	0	13.6	955	1510	673
Chase	0.92	13.6	76.36	120.80	53.84
Rest	7.37	0	0.019	0.0455	0.00038
Withdrawal	7.51	13.8			
KFM01D 377					
Injection	0	13.8	1040	1570	665
Chase	0.89	13.8	84.90	128.16	54.29
Rest	7.33	0	0.06	0.0508	0.00032
Withdrawal	8.63	13.8			

Table 4. Inferred diffusion and sorption parameters for the three SWIW tests.

Test	ϕ_m		$2r_m$ (m)	Effective contact area	Rb $K_d\rho_p$		Cs $K_k\rho_p$	
	Finite	Semi-infinite	Finite	Finite	Finite	Semi-infinite	Finite	Semi-infinite
Two-population models								
KLX11A 598-599 m	0.278	0.0064	0.0178	0.2	7	7	3	3
KFM01D 431-432 m	0.07	0.0056	0.007	0.2	1.5	1.5	5	5
KFM01D 377-378 m	0.07	0.0032	0.011	0.2	1	1	1	1
Single-population model								
KFM01D 431-432 m		0.0056*				2		20

*matches the BTC tail only; to match the peak only $\phi_m = 0.02$

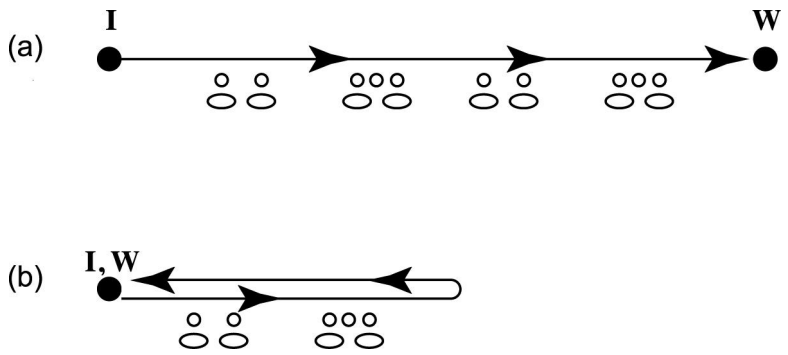

Figure 1. Schematic diagram of particle travel path during a two-well test (a) and a SWIW test (b). Arrows represent advection through the fracture and circles and ovals represent finite rock blocks into which diffusion and sorption may occur. The semi-infinite rock matrix, also present, is not shown in this figure. I and W indicate injection and withdrawal wells respectively.

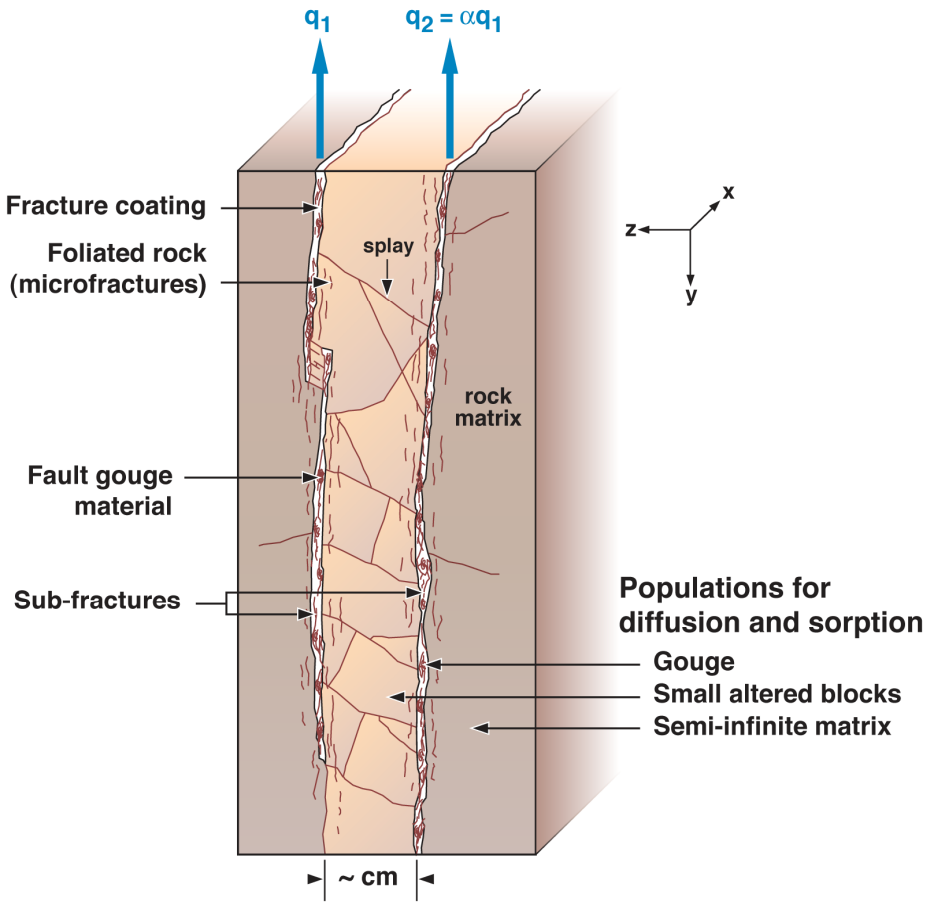

Figure 2. Complex fracture model (Tsang and Doughty, 2003; Mazurek et al., 2001).

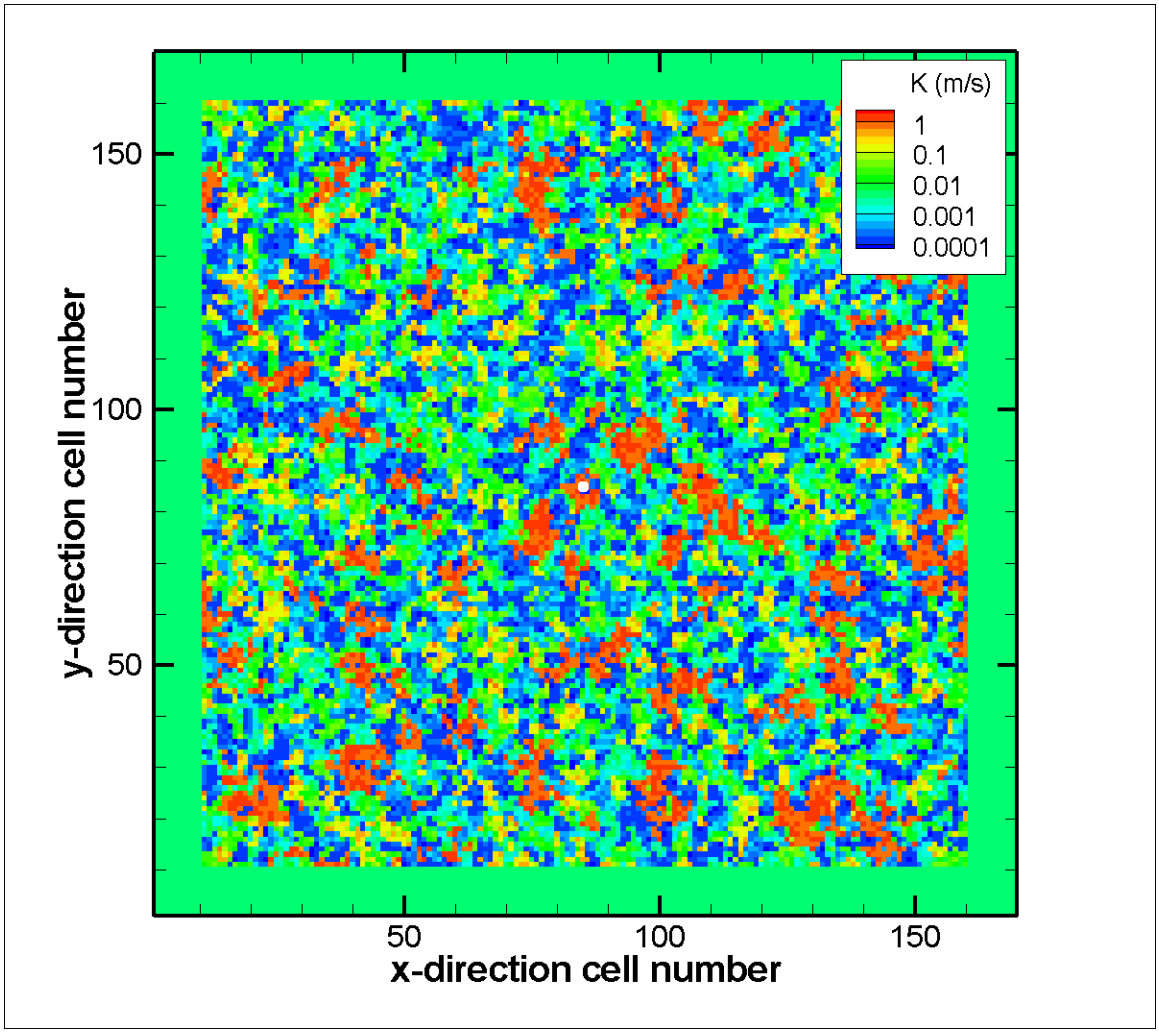

Figure 3. Simulated fracture hydraulic conductivity K distribution, with $K = T/b$ where T is transmissivity and b is aperture, obtained using the parameters given in Table 1.

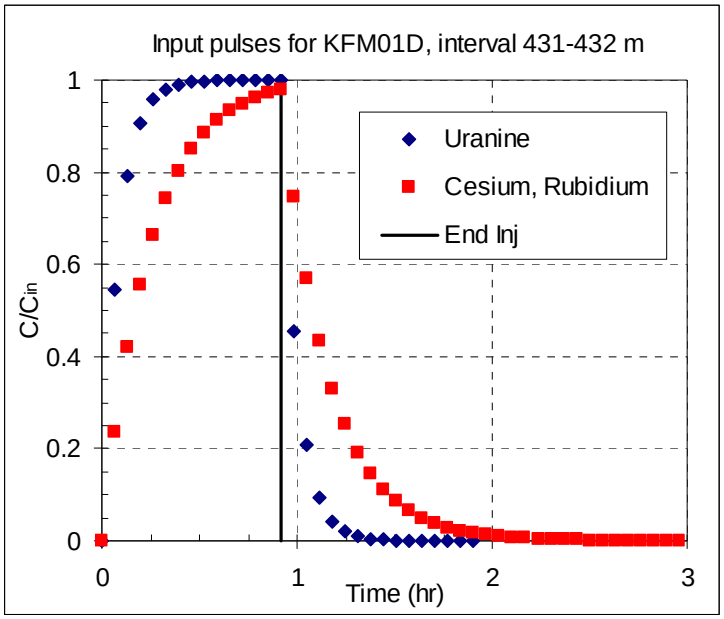

Figure 4. Example of time-dependent tracer concentration entering the fracture.

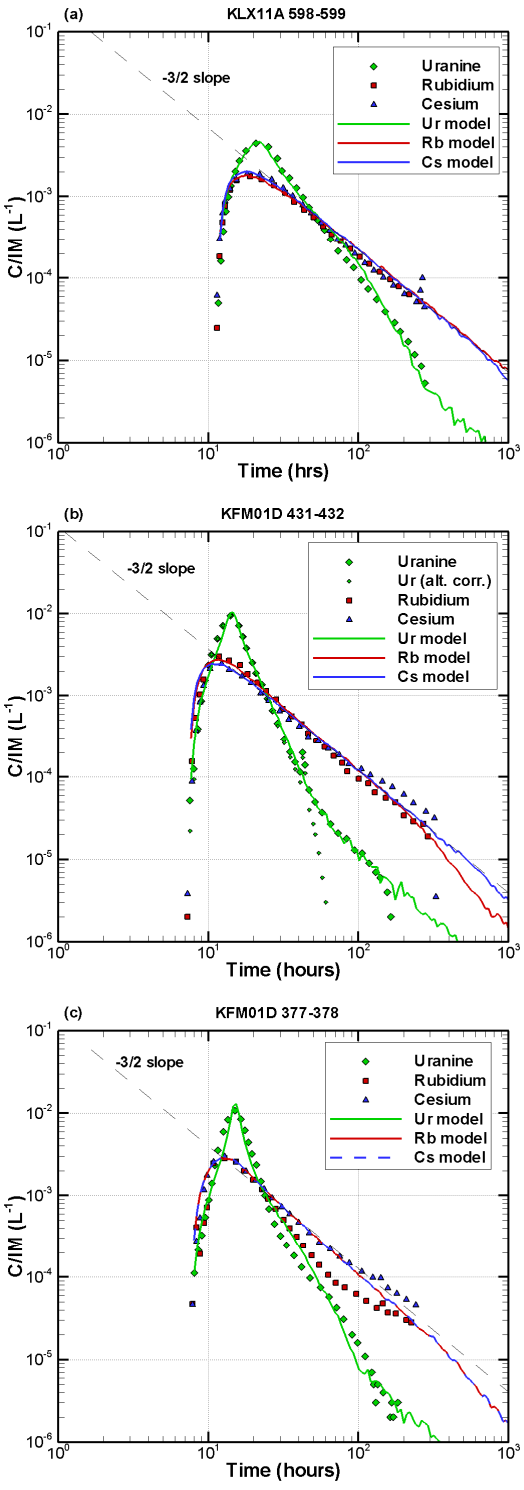

Figure 5. Tracer BTCs for (a) test KLX11A, interval 598-599 m; (b) test KFM01D, interval 431-432 m; (c) test KFM01D, interval 377-378 m. Tracers have been corrected for background concentration. Field data is shown with symbols, model results with lines. The dashed line with -3/2 slope is added for reference. For KFM01D interval 431-432 the alternative background correction discussed in Section 5 is shown with small symbols.

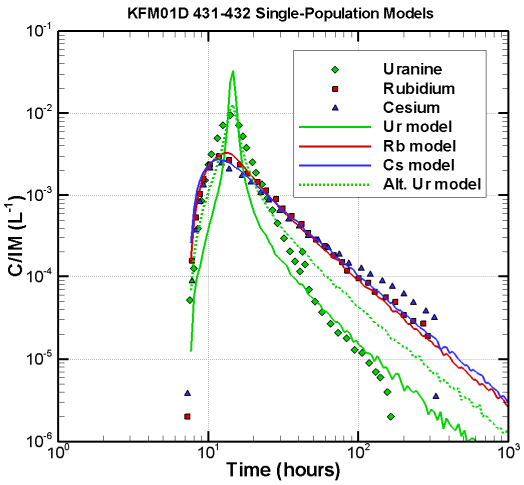

Figure 6. BTCs for Test KFM01D, interval 431-432 m, using models with only a single semi-infinite population for diffusion and sorption.